energies

MDPI

Article

Water Heating and Operational Mode Switching Effects on the Performance of a Multifunctional Heat Pump

Win Jet Luo [1], Kun Ying Li [1,*], Jeng Min Huang [2] and Chong Kai Yu [2]

[1] Graduate Institute of Precision Manufacturing, National Chin-Yi University of Technology, Taichung 41170, Taiwan; wjluo@ncut.edu.tw

[2] Department of Refrigeration, Air Conditioning and Energy Engineering, National Chin-Yi University of Technology, Taichung 411, Taiwan; jmh@ncut.edu.tw (J.-M.H.); ychongkai@gmail.com (C.-K.Y.)

* Correspondence: likunying@ncut.edu.tw; Tel.: +886-42392-4505 (ext. 6490)

Received: 21 August 2020; Accepted: 10 September 2020; Published: 18 September 2020

Abstract: In this study, a multifunctional air and water source heat pump system was developed with a parallel refrigerant piping arrangement, which possessed six operational functions: space cooling (SC), space heating (SH), water heating (WH), water cooling (WC) and two composite operational modes. The two composite operational modes were the SC/WH mode and the SH/WH mode. The performance of the multifuctional heat pump system under different ambient conditions was investigated based on the testing standards of CNS 14464 and CNS 15466. In this study, the effect of the direct water heating (DWH) and circulating water heating (CWH) methods on the performance was investigated. It was found that the water heating performance of the system by the DWH method is better than that of the system by the CWH method. The water heating capacity and $COP_{w,h}$ of the DWH method can be improvement by 2.6% to 22.1% and 2.9% to 50.8%, respectively. Moreover, this study developed a refrigerant pressure balance method to achieve an effective steady state of the refrigerant pressure after operational mode switching. By the refrigerant pressure balance method, the required time to attain the steady state could be greatly reduced—by 50%. However, the deviation of the refrigerant mass flow rate between the refrigerant pressure balance method and the refrigerant pump down method after operational mode switching ranged from 0.15% to 7.6%.

Keywords: multifunctional heat pump; coefficient of performance; composite operational mode; Direct heating; Circulating heating

1. Introduction

With the depletion of fossil fuels and global warming problems, governments worldwide are pursuing energy saving strategies to reduce energy consumption. In recent years, heat pumps have been considered an effective approach for energy saving purposes and have gradually been adopted in residential buildings and industrial applications.

At present, heat pump technology has been developed for several decades to reduce the energy consumption in residential and commercial buildings. In recent years, heat pumps have been widely applied, not only in applications for medium- and high-energy consumption users but also in broad applications in hospitals, hotels, schools, swimming pools, nursing homes, and households for hot water generation [1–3]. The heat pump was originally a single-function heating system and discharged cold energy to the ambient environment. According to the method of heat extraction, the heat pump for water heating (WH) is mainly divided into two types: water to water and air to water pumps. A large proportion of residential buildings are designed with conventional heaters that consume fossil

fuels or electricity, which may cause carbon dioxide emission problems and low-efficiency operating conditions. However, regarding the heating performance, the heat pump system is much greater than the conventional electrical heater [4,5]. Regarding the heat recovery and thermal storage in the heat pump system, the wasted heat ejected from condenser of an air conditioner can be recovered and be used to generate hot water. In the past 70 years, several studies have found that high-performance heat pumps can be employed to achieve energy savings [6–10]. However, these studies have mainly focused on energy savings in terms of the hot water supply. In addition to hot water generation, a heat pump system can be designed to perform various operational functions including space cooling, space heating, hot water generation and other composite functions [11,12]. Hitunnen et al. [13] utilized EnergyPRO software to simulate the recovered waste energy of heat source from heat pump. The results of the simulation show that increasing the waste heat utilization by a different strategy, such as cost and CO_2 emission, mostly influence the utilization of other renewable and low-carbon heat sources. Gong et al. [14] proposed a new heat recovery technology that combines air cooling and water cooling methods to replace the traditional air-conditioning heat pump system with space cooling. This system utilizes the fluid bypass pneumatic control method for operational mode shifting. From experiments, it is found that the new air-conditioning heat pump system can operate stably and efficiently with a coefficient of performance (*COP*) of 6.0. Liu et al. [15] developed a vapor injection heat pump and investigated the performance of the heat pump under different driving frequencies of the compressor and primary temperatures. It was found that the heating capacity and heating performance of the heat pump can be increased and the discharging temperature of the compressor can be reduced by the vapor injection. León-Ruiz et al. [16] proposed an analytical model to investigate the performance of a Direct Expansion Solar-Assisted Heat Pump and compared three experimental results in literature. By the analytical analysis, an optimization operational strategy was established to improve the performance of the system. Xu et al. [17] recommended two different air–water dual-source composite evaporators to enhance the thermal efficiency. Through the different composite evaporator designs, a high *COP* and hot water temperature can be obtained. In the heating mode, combined with air and water sources, the hot water temperature is increased from 18.1 °C to 51.1 °C, and the overall performance increases from 8.8% to 13.3%. Liu et al. [18] designed a thermal storage heat pump utilizing a dual evaporator and phase change material in the secondary evaporator. The COP value of the heat pump can be enhanced by 0.85% to 4.72%. In other words, energy savings can be achieved with a multifunctional and well-integrated system.

In recent years, multifunctional heat pumps have been developed to avoid energy waste, and the recovered energy can be used for other purposes to expand the applications of heat pump systems. To avoid wasting energy and reuse recovered energy, Ji et al. [19] developed a multifunctional domestic heat pump (MDHP) system combined with a heat pump water heater and a household air conditioner. The results indicated that the new system could save energy through multiple duties and can work stably under prolonged operation in regions with mild winter temperatures. The system can operate stably at an ambient temperature of 2.8 °C. Liang et al. [20] designed a multifunctional air source heat pump with cooling, heating and hot water supply functions. The system performance variations regarding the hot water supply under different temperature conditions were analyzed. Their experimental results showed that the *COP* of the multifunctional heat pump increases with increasing ambient temperature, and the *COP* can reach 4.1 under higher-temperature conditions.

Liu et al. [21] proposed a heat pump system that effectively recovers waste heat from wastewater for residential building heating and cooling. Compared to their previous prototype unit [22], the space cooling capacity is increased 20.7% in the space cooling operational mode, and the space cooling capacity can be increased 21.51% in the hot water operational mode. In addition to attaining a high thermal efficiency, heat pump systems also exhibit an excellent energy saving performance.

Regarding the heat exchanger arrangement for heat recovery, Liu et al. [5] investigated the heating performance of a proposed composite multifunctional heat pump system. With the air and water sources arranged in parallel, the developed system attains the best performance in the space heating

(SH) mode and in the SH and WH composite mode. The heating capacity of the system in the composite mode is lower than that of the system in the single SH mode. However, the total *COP* in the composite mode is higher than that in the single heating mode, and the difference in heating capacity between the two modes is smaller than 12%. Liu et al. [22] developed a type of multifunctional water source heat pump system that generates hot water through two-stage heating in the heating mode. Their experimental results showed that 15.4–57% of the condensing heat can be recovered in cooling and heat recovery. The developed system, operating with a large hot water temperature difference in the heating mode, can achieve a high heating performance. Liu et al. [23] proposed another composite multifunctional heat pump system and compared it to the traditional air source heat pump system. The multifunctional heat pump system achieved a superior performance in the cooling mode. It was found from the results that the combination of heat sinks would affect the cooling capacity and *COP* value of the system. Luo et al. [24] developed a multi-functional heat pump with a plate heat exchanger and a condenser in parallel arrangement in order to reclaim more waste heat in operation. The performance of the multi-functional heat pump was investigated in various seasonal operational modes. The average water heating performance can attain values of 3.77 and 1.91 in summer and winter operational modes, respectively.

For the performance and operation of a multifunctional heat pump system, the water heating and refrigerant pressure build-up methods are two major concerns for engineers. In the literature, the effect of the water heating method on the performance of a multifunction heat pump is less investigated. Moreover, the refrigerant pressure build-up method, after switching operational mode on the operations and performance of the multifunctional heat pump with parallel refrigerant piping design, has never been studied. In order to enhance the performance of the developed multifunctional heat pump and effectively build up the refrigerant pressure difference in the refrigerant cycle after operational mode switching, the effect of a novel refrigerant pressure balance control method and water heating method were investigated.

In this study, a new multifunctional heat pump system is developed that possesses six operational functions, including space cooling (SC), space heating (SH), water heating (WH), water cooling (WC), the SC and WH composite (SC/WH) mode and the SH and WH composite (SH/WH) mode. To recover more energy and attain a high operational performance, the heat exchangers for heating and cooling in the refrigerant cycle are designed with a parallel arrangement. The performance of the system in the different operational modes was investigated. Regarding the WH operational mode of the developed system, the effect of two water heating methods, i.e., the DWH and CWH methods, on the performance of the system was investigated as well. Moreover, to build up the refrigerant pressure difference in the refrigerant cycle and reduce the required time to attain the steady state after operational mode switching, the effect of a novel refrigerant pressure balance control method was investigated.

2. System Design and Experimental Method

The performance of the system in the different operational modes was investigated. Figure 1 shows the flowchart of this study. At the beginning stage of the experiment, the superheat degrees to attain a suitable cooling capacity of the heat pump system under the different operational conditions is studied. Then, through the experimental measurements, the performance analysis of the developed system in different operational modes is investigated. Finally, the water heating methods and refrigerant pressure build-up methods on the performance of the developed system is investigated.

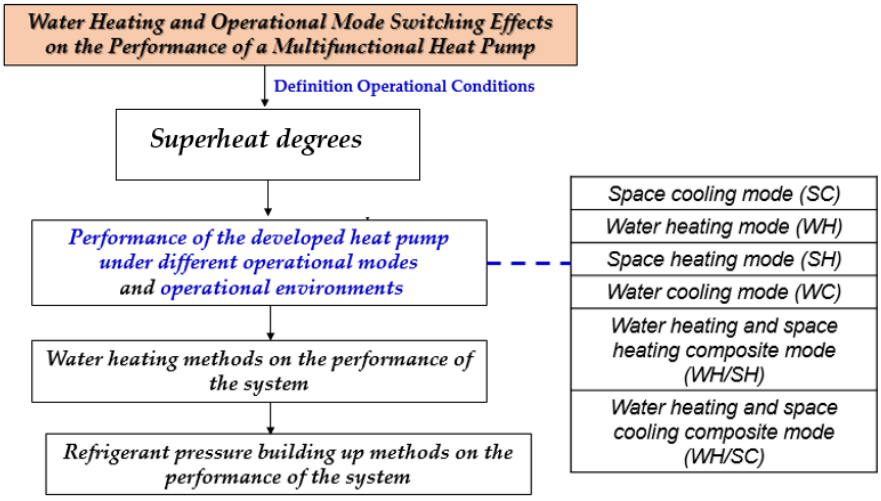

Figure 1. Experimental flowchart of this study.

In the study, the flowmeter in this study was manufactured by Jetec electronics Co., Ltd. in Taiwan and the type is NW20-NTN. The measuring range of the flowmeter was 3–60 L/min, and the accuracy value was ±2%. The pressure transducers were manufactured by ATLANTIS Co., Ltd. in Taiwan and the type was DS-LJ121. The pressure measurement range was 0–40 $kg/cm^2 \pm 0.25\%$. The thermal meter was a PT100 thermometer. The type was an E52-P15AY, which was made by OMRON. The measurement accuracy was 0–1200 °C ± 1%. The compressor power was calculated after measuring the power consumption, operating voltage, operating current and power factor. The parameter measurement equipment was manufactured by DELTA Electronics, Inc. in Taiwan and the type was a DPM-C530. The measurement accuracy was ±0.5%. The power consumption can be obtained according to the equation: $P = \sqrt{3}V \times I \times \cos\theta$ (P is the compressor operating power; V is the operating voltage; I is the operating current; $\cos\theta$ is the power factor). The mass flow rate of refrigerant was measured with a refrigerant mass flow meter. The refrigerant mass flow meter was manufactured by Bronkhorst in the United States and the type was an M15-AGD-99 with accuracy of 3–300 kg/h ± 0.2%. The air volume measuring device was manufactured by TES electronics Corp. in Taiwan and the type was a TES-3142. The measurement accuracy was ±1%. The humidity meter was manufactured by TES electronics Corp. in Taiwan and the type was a TES-1162. The measurement accuracy was ±1.8%RH.

According to Kline [25], the total uncertainty can be attained by the equation $\Delta y = [(\Delta x_1)^2 + (\Delta x_2)^2 + \ldots + (\Delta x_n)^2]^{1/2}$, where $\Delta x_1, \Delta x_2, \ldots, \Delta x_n$ are the uncertainties in the corresponding variables. In this study, the total uncertainty associated with the coefficient of performance was found to be ± 3.1%. The uncertainty of $COP_{s,c}$ equals to that of $COP_{s,h}$ with a value of ±2.3%. The uncertainties in measuring the $COP_{s,c}$ and $COP_{s,h}$ can be obtained from the measurement errors of the flowmeter, compressor power measurement and air volume measuring devices. However, the uncertainty of $COP_{w,c}$ equals to that of $COP_{w,h}$ with a value of ±2.5%. The uncertainties in measuring the $COP_{w,c}$ and $COP_{w,h}$ can be obtained from the measurement errors of the flowmeter, compressor power measurement, temperature sensor and water volume measuring device.

Figure 2 shows the configuration design of the multifunctional heat pump, which consists of two fin-tube heat exchangers, two plate heat exchangers, two electronic expansion valves, one four-way valve and several solenoid valves. The plate heat exchanger (PHX II) and fin-tube heat exchanger (FTHX II) were employed in parallel arrangement to conduct heat exchange for WH and SH purposes, respectively. However, the PHX I and FTHX I in the parallel arrangement were used to conduct heat exchange for WC and SC purposes, respectively. The plate heat exchanger and fin-tube heat exchanger are the K070S-22C-S5P8 type and the HERAN HO-502H type, which are manufactured by Kaori and HERAN, Taiwan, respectively. The maximum working temperature and flow rate of

the K070S-22C-S5P8 type are 200 °C and 240 LPM, respectively. The maximum working pressure and heat transfer power of the K070S-22C-S5P8 type are 45 Bar and 17.58 kW, respectively. The maximum working temperature and flow rate of the HERAN HO-502H type are 200 °C and 240 LPM, respectively. The maximum working pressure and the heat transfer power of the HERAN HO-502H type are 30 Bar and 17.58 kW, respectively. The refrigerant used in this study was R-410A. R-410A is composed of two azeotropic mixtures which are composed of hydrogen, fluorine and carbon elements. The characteristics of R-410A are stability, non-toxicity and superior performance. The performance of air conditioners can be improved by using a R-410A refrigerant.

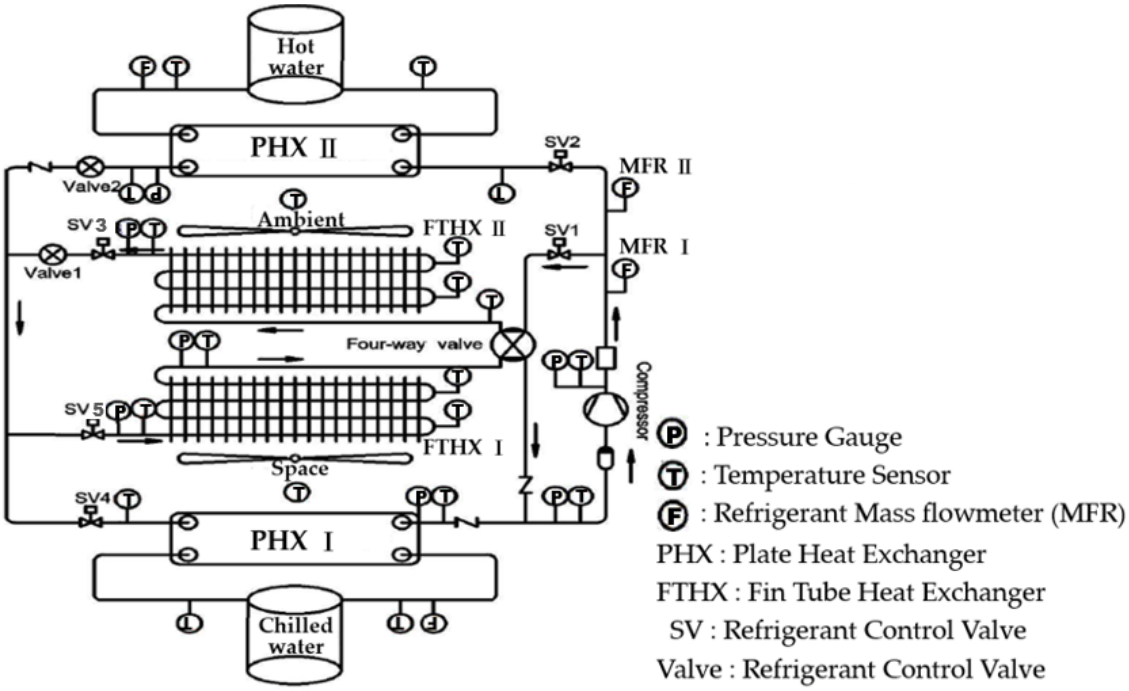

Figure 2. Configuration of the multifunctional heat pump system.

2.1. Operational Modes of the Heat Pump System

1. Space cooling mode (SC mode)

As shown in Figure 3a, in the SC mode, solenoid valves SV2 and SV4 are turned off, and solenoid valves SV1 and SV3 are turned on. The red line denotes the high refrigerant pressure side and the blue line denotes the low refrigerant side in the refrigerant piping system. The refrigerant vapor from the low-pressure evaporator is compressed into high-pressure superheated vapor by the compressor, and the refrigerant vapor is then condensed into a subcooled liquid refrigerant by emitting condensation heat into the ambient environment from the condenser (FTHX II, Fin Tube Heat Exchanger II). Afterwards, the pressure of the subcooled liquid refrigerant is reduced by passing through an expansion valve (valve 1), and the refrigerant then enters the evaporator. In the evaporator, the low-pressure refrigerant absorbs heat from the space and evaporates into refrigerant vapor, resulting in a cooling effect in the air-conditioning space. The resulting refrigerant vapor from the evaporator returning to the compressor completes the refrigeration cycle.

2. Water heating mode (WH mode)

In the WH mode, as shown in Figure 3b, solenoid valves SV1, SV2 and SV3 are activated, and solenoid valves SV4 and SV5 are deactivated. The evaporative heat of the refrigerant is absorbed from the ambient environment in the FTHX II on the low-refrigerant pressure side, and the high-pressure superheated refrigerant vapor discharged from the compressor condenses in the PHX II (Plate Heat

Exchange II). The condensation heat is recovered by the circulating water in the PHX II to generate hot water, which is stored in the hot water tank. The pressure of the subcooled liquid refrigerant is reduced after passing through the expansion valve (valve 1) and then enters the FTHX II again.

3. Space heating mode (SH mode)

In the SH mode, as shown in Figure 3c, solenoid valves SV1, SV3 and SV5 are switched on, and solenoid valves SV2 and SV4 are switched off. The switch in refrigerant flow direction by the four-way valve leads the refrigerant to absorb heat from the ambient environment and is evaporated into vapor in the FTHX II, after which condensation heat is emitted into the space, while the refrigerant vapor condenses into liquid in the FTHX I (Fin Tube Heat Exchanger I) on the high-pressure side.

4. Water cooling mode (WC mode)

As shown in Figure 3d, the SV1, SV3 and SV4 valves are turned on, but the SV2 and SV5 valves are turned off. The refrigerant in the PHX I (Plate Heat Exchange I) absorbing evaporative heat from the circulating water is evaporated into vapor to generate chilled water. The high-temperature and high-pressure refrigerant discharged from the outlet port of the compressor condenses into liquid and emits condensation heat into the ambient environment by the FTHX II. The pressure of the condensing liquid refrigerant is reduced by passing through expansion valve 1 and returning to the FTHX I.

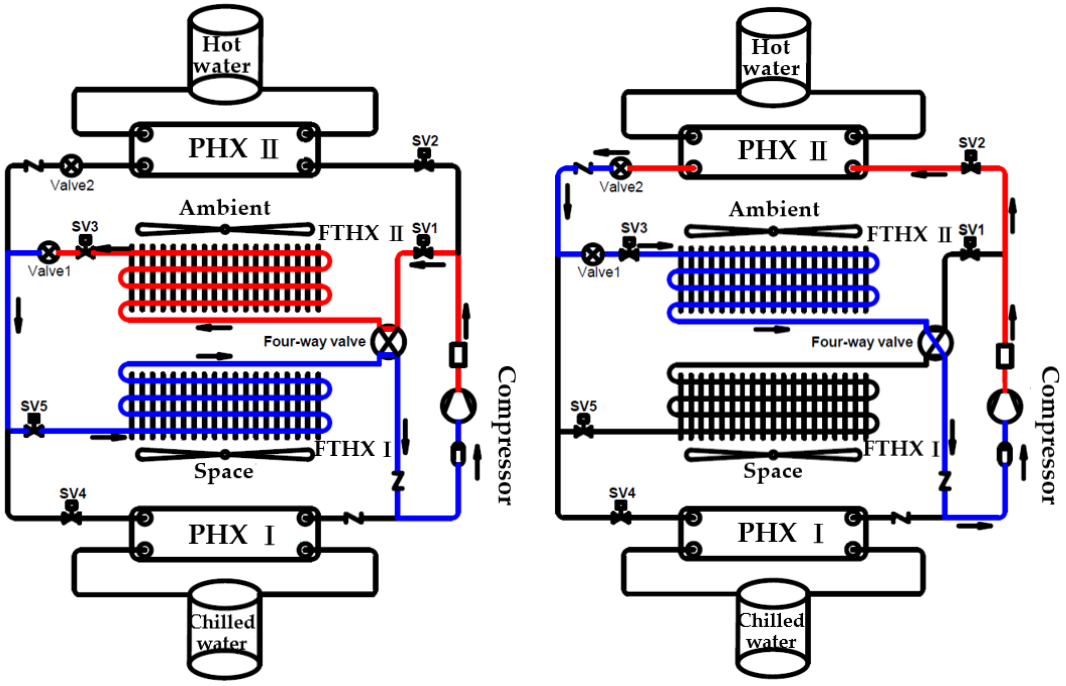

(**a**) (**b**)

Figure 3. *Cont.*

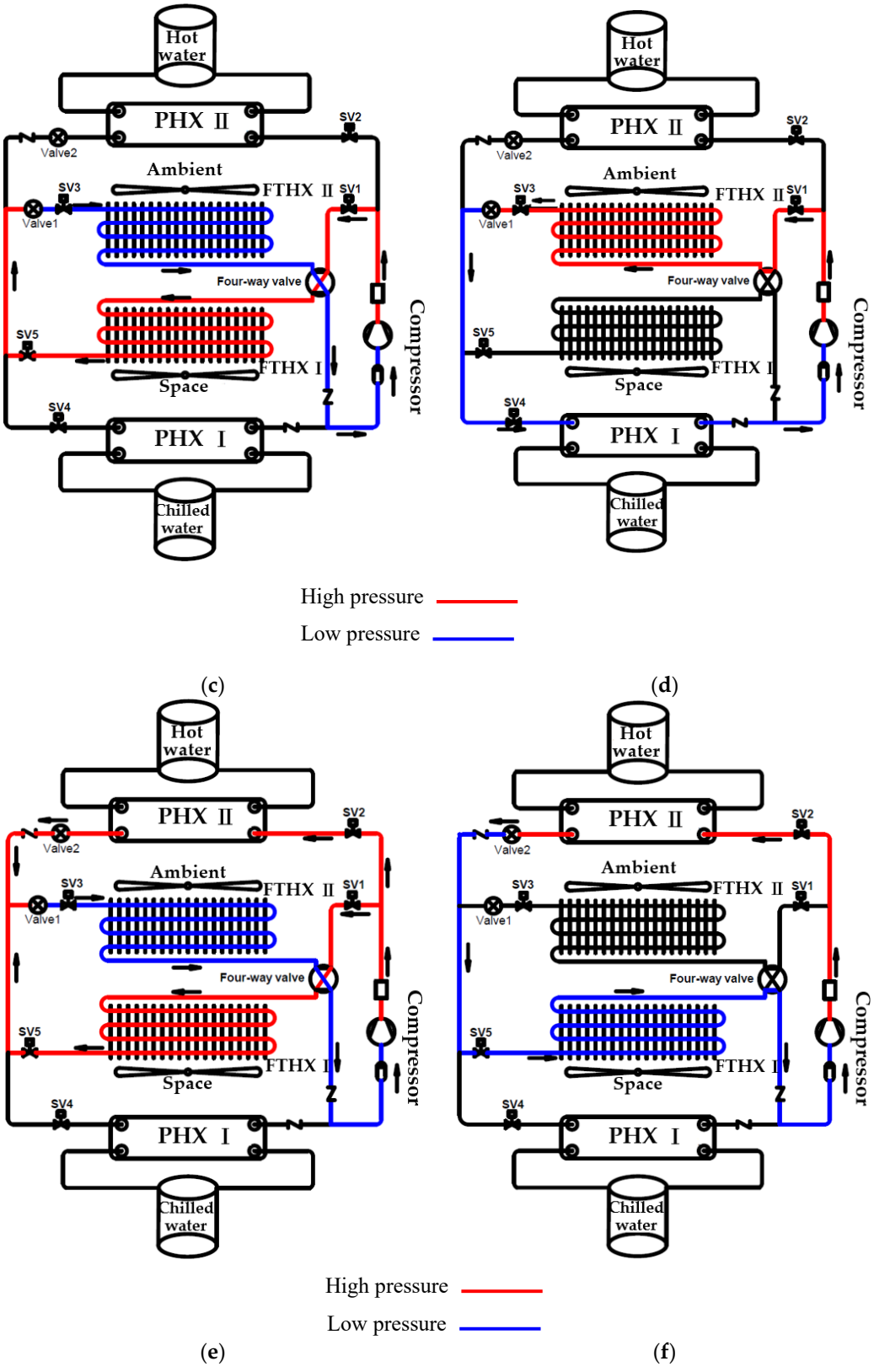

Figure 3. Operational Modes of the Heat Pump System. (**a**) Refrigerant flow route in the space cooling (SC) mode. (**b**) Refrigerant flow route in the water heating (WH) mode. (**c**) Refrigerant flow route in the space heating (SH) mode. (**d**) Refrigerant flow route in the water cooling (WC) mode. (**e**) Refrigerant flow route in the WH/SH mode. (**f**) Refrigerant flow route in the WH/SC mode.

5. Water heating and space heating composite mode (WH/SH mode)

In the WH mode, as shown in Figure 3e, the SV1, SV2, SV3 and SV5 valves are switched on, but the SV4 valve is switched off. Heat is absorbed from the ambient environment by the FTHX II, and condensation heat is recovered by the circulating water in the PHX II and is emitted into the space for heating by the FTHX I on the high-refrigerant pressure side.

6. Water heating and space cooling composite mode (WH/SC mode)

In the WH and SC composite mode, as shown in Figure 3f, the SV2 and SV5 valves are activated, but the SV1, SV3 and SV4 valves are deactivated. Heat is absorbed from the ambient environment by the low-pressure PHX I for SC, and condensation heat is recovered by the circulating water in the high-pressure PHX II for water heating.

In the SH/WH mode, the vapor refrigerant discharging from the compressor can be introduced into PHX II and FTHX I due to the parallel piping arrangement. Because the pressure drops in the PHX II and FTHX I are different, the openness of expansion valve 2 is manually adjusted to equalization of the refrigerant pressure of the two refrigerant streams from PHX II and FTHX I before entering expansion valve 2.

In the WH and WH/SH operational modes, the condensing refrigerant from PHX II after passing through expansion valves, V1 and V2 becomes low pressure refrigerant, then flows into FTHX II for evaporation. The openness of the expansion valves, V1 and V2 are manually adjusted in order to maintain a suitable evaporation pressure and a superheat degree in the refrigeration cycle.

Table 1 shows the corresponding electromagnetic valve actions in the different modes of refrigerant circulation.

Table 1. Actions of the solenoid valves, expansion valves and four-way valves in the different operational modes.

Operational Mode	Action State							
	RV Four-Way Valve	SV1	SV2	SV3	SV4	SV5	V1	V2
SC		ON		ON		ON	ON	
SH	ON	ON		ON		ON	ON	
WH	ON		ON	ON			ON	ON
WC		ON		ON	ON		ON	
WH/SH	ON	ON	ON	ON		ON	ON	ON
WH/SC			ON			ON		ON

2.2. Heat Exchange Theory of Heat Pump

The instant cooling and heating capacities of the heat pump system in the different operational modes are:

$$Q_{s,c} = \dot{m}_{s,c} C_p (T_{sco} - T_{sci}), \quad (1)$$

$$Q_{s,h} = \dot{m}_{s,h} C_p (T_{sho} - T_{shi}) \quad (2)$$

$$Q_{w,c} = \dot{m}_{w,c} C_p (T_{wco} - T_{wci}) \quad (3)$$

$$Q_{w,h} = \dot{m}_{w,h} C_p (T_{who} - T_{whi}) \quad (4)$$

where $Q_{s,c}$ is the instant space cooling capacity, $Q_{s,h}$ is the instant space heating capacity, $Q_{w,c}$ is the instant water cooling capacity, $Q_{w,h}$ is the instant water heating capacity, $\dot{m}_{s,c}$ $\dot{m}_{s,h}$ are the air flow rates in space cooling and heating, $\dot{m}_{w,c}$ and $\dot{m}_{w,h}$ are the water flow rate in water cooling and heating,

C_p is the specific heat of water, T_{sco} and T_{sho} are the air temperatures at the outlet of the FTHX, T_{sci} and T_{shi} are the air temperatures at the inlet of the FTHX in space cooling and space heating, respectively, T_{wco} and T_{who} are the water temperatures at the outlet of the PHX and T_{wci} and T_{whi} are the water temperatures at the inlet of the PHX in water cooling and water heating, respectively.

Within an operating period of duration τ, average coefficient of performance for space heating ($COP_{s,h}$) and average coefficient of performance for space cooling ($COP_{s,c}$) can be expressed as:

$$COP_{s,c} = \frac{\int_0^\tau Q_{s,c}(t)dt}{\int_0^\tau W(t)\,dt} \tag{5}$$

$$COP_{s,h} = \frac{\int_0^\tau Q_{s,h}(t)dt}{\int_0^\tau W(t)\,dt} \tag{6}$$

where $Q_{s,h}$ is the instant heating capacity for space heating, $Q_{s,c}$ is the instant cooling capacity for space cooling and W is the instant required power for the compressor.

The average coefficient of performance for water heating ($COP_{w,h}$) and the average coefficient of performance for water cooling ($COP_{w,c}$) can be expressed as:

$$COP_{w,c} = \frac{\int_0^\tau Q_{w,c}(t)dt}{\int_0^\tau W(t)\,dt} \tag{7}$$

$$COP_{w,h} = \frac{\int_0^\tau Q_{w,h}(t)dt}{\int_0^\tau W(t)\,dt} \tag{8}$$

where $Q_{w,h}$ is the instant heating capacity for water and $Q_{w,c}$ is the instant cooling capacity for water.

The average coefficient of performance for space cooling/water heating ($COP_{t,sc/wh}$) and the average coefficient of performance for space heating/water heating ($COP_{t,sh/wh}$) can be expressed as:

$$COP_{t,sc/wh} = COP_{s,c} + COP_{w,h} \tag{9}$$

$$COP_{t,sh/wh} = COP_{s,h} + COP_{w,h} \tag{10}$$

2.3. Performance Measurements of the Heat Pump System

Based on the measurement and verification standards of CNS 15466 and CNS 14464, the performance of the developed heat pump system under the different operational conditions and operational modes was investigated, as summarized in Table 2. The heating performance of the developed heat pump system with the DWH and CWH methods was investigated in the different operational modes based on the standard of CNS 14464. In this study, in the operational modes with water heating, the supplied water temperature to the PHX I is maintained at 15 °C, and the design water temperature after heating is 55 °C. The operational conditions under the DWH (Direct Water Heating) and CWH (Circulating Water Heating) methods are listed in Table 3.

Regarding the WH methods in PHX II, two heating methods were adopted in this study, namely, the DWH and CWH methods. In the CWH method, the circulating water flowing in a closed loop is continuously heated by the refrigerant condensation in the PHX II until the water temperature in the water storage tank attains the design water temperature. However, in the DWH method, the water flow rate in the closed loop can be adjusted to directly reach the design water temperature after heating by the PHX II.

The performance of the developed system is measured in an environmental control laboratory with a TAF certificate (Taiwan Accreditation Foundation), which shows the required environmental conditions for the measurement. In this study, the FTHX I and FTHX II are installed in different

individual environmental chamber with controlled constant temperature and constant humidity with temperature deviation of ±0.5 °C A normative water tank can supply constant water temperature to the developed heat pump system for measurement with water temperature deviation of ±0.1 °C Figure 4 shows a schematic diagram of the performance measurement environment.

Table 2. Operational conditions for performance investigations in different operational modes.

	Air Conditioning Space		Ambient Environment		Water Side	
	T_{db} (°C)	T_{wb} (°C)	T_{db} (°C)	T_{wb} (°C)	Water Inlet Temperatures (°C)	Water Outlet Temperatures (°C)
SC	27	19	35	24	N/A	
SH	20	15	7	6	N/A	
WH	N/A	N/A	20	15	15	55
WC	N/A	N/A	20	15	12	7
WH/SH	20	15	7	6	9	55
WH/SC	27	19	N/A	N/A	15	55

Table 3. Operational conditions for the different water heating methods.

Hot Water Type	Mode	Indoor Temperature (°C)	Outdoor Temperature (°C)	Water Inlet Temperatures (°C)	Water Outlet Temperatures (°C)	$COP_{w,h}$
Direct heating and Circulating heating	WH	N/A	20(T_{db}) 15(T_{wb})	15	55	3.19
		27 (T_{db}) 19 (T_{wb})	N/A	15	55	4.58

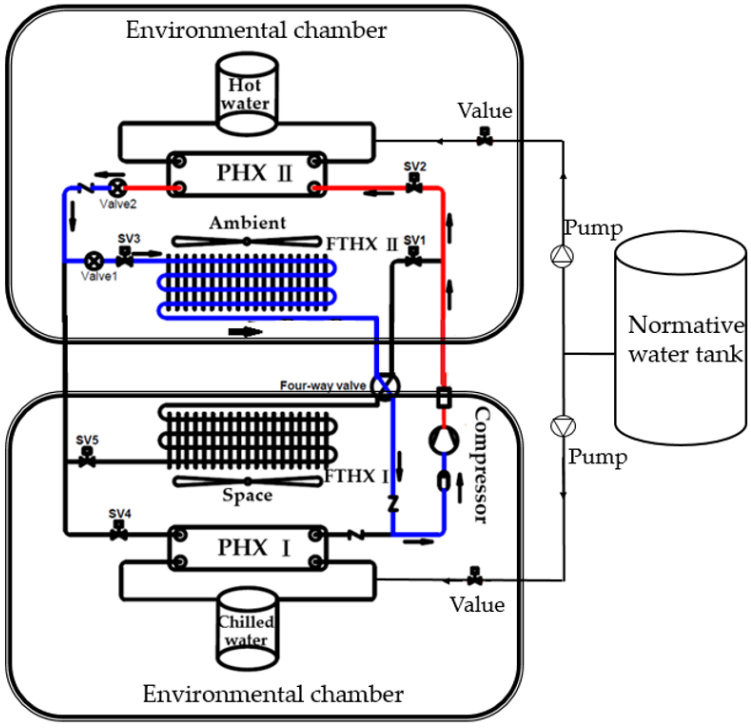

Figure 4. Schematic diagram of the performance measurement environment.

In order to ensure the steady state condition and the measurement accuracy, the performance measurements follow the procedures below.

Directions for the Water Heating Method:

1. Confirm that the normative water tank is full and the initial average water temperature reaches the rated conditions.
2. Connect the PHX II of the developed heat pump system with the normative water tank, and turn on the valves between the developed system and normative water tank.
3. Turn on the water pump and make the water from the normative tank flow through PHX II. The developed heat pump system is automatically triggered and continues operating.
4. Adjust the water flow rate from the normative tank to PHX II to make the outlet water temperature from PHX II to reach the required water temperature.
5. After the developed system reaches a steady state under the specified conditions for one hour, measure the water volume from the normative tank to PHX II, inlet and outlet water temperatures of PHX II and power consumption of the developed system every 5 min.
6. After the outlet water volume reaches the required value and after collecting at least seven sets of measurement data, the heating capacity and performance coefficient of the developed system can be obtained from Equations (4) and (8).

Directions for the Circulating Water Heating Method:

1. Confirm that the normative water tank is full and the initial average water temperature reaches the rated conditions.
2. Connect the empty hot water tank of the developed heat pump system with the normative water tank, and turn on the valves between the developed system and normative water tank.
3. Turn on the water pump and make the water from the normative tank fill the hot water tank of the developed system. Confirm that the hot water tank of the developed system is full and the initial average water temperature reaches the rated conditions.
4. Turn on the water pump and make the water from the hot water tank flow through PHX II for heating, then return to the hot water tank. Confirm that the circulating water flow rate between PHX II and hot water tank attains the required value and steady state.
5. The developed heat pump system is triggered and continues operating, and measures the water volume from PHX II, inlet and outlet water temperatures of PHX II and power consumption of the developed system every 10 s until the water temperature in the hot water tank attains the required temperature.
6. Calculate the heating capacity and performance coefficient of the developed system through Equations (4) and (8).

In this study, water cooling measurement procedures are similar to those for water heating, and the circulating water cooling method was adapted.

3. Results and Discussions

3.1. Superheat Degree Effect on the Cooling Capacity and Power Consumption

Figure 5 shows the air cooling capacity and power consumption of the compressor at different degrees of superheat of the refrigerant cycle. As shown in the figure, the power consumption of the compressor gradually decreases with an increasing superheat degree because less refrigerant is introduced into the evaporator by reducing the openness of the expansion valve under high-superheat degree conditions with increasing superheat degree of the refrigeration cycle. However, in terms of the cooling capacity, a peak value occurs at a superheat degree of 5 °C. To maintain a suitable cooling capacity of the system under the different operational conditions, a superheat degree of 5 °C of the refrigeration cycle is maintained in the following experiments.

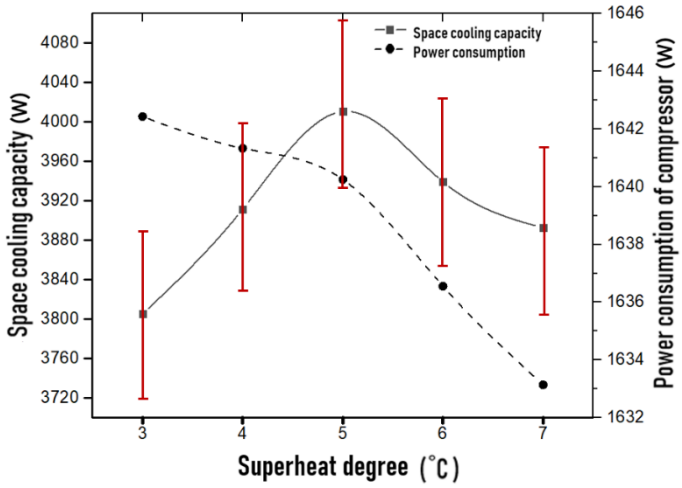

Figure 5. Space cooling capacity and power consumption of the compressor at the different superheat degrees.

The effect of the superheat degree of the refrigeration cycle on the cooling capacity and the required power consumption of the compressor in the space cooling operational mode is investigated under an ambient environmental conditions of T_{db} = 35 °C and T_{wb} = 24 °C and indoor space setting conditions of T_{db} = 27 °C and T_{wb} = 19 °C. In the space cooling experiments, the solenoid valves of SV1, SV3 and SV5 are turned on, and the superheat degree of the refrigeration cycle is controlled by adjusting the openness of the expansion valve, V1. By reducing the openness of the expansion valve, V1, the refrigeration mass flow rate in the refrigeration cycle is reduced as well. However, the evaporation of the liquid refrigerant in the evaporator can be completed in an area with less heat transfer due to a smaller refrigerant mass flow rate; thus, the superheat degree and refrigeration effect of the refrigeration cycle can be increased. The cooling capacity is proportional to the refrigerant mass flow rate and refrigeration effect. Increasing the superheat degree can increase the refrigeration effect of the refrigeration cycle but reduce the refrigerant mass flow rate in the refrigeration cycle. Thus, for the developed system in space cooling mode, a peak value exists at the superheat degree of 5 °C. The distributions of cooling capacity and required power at five different superheat degree points are shown in Figure 5. The increase percentage of the space cooling capacity between the peak value and minimum value is about 2.7%. The uncertainty of the space cooling capacity is ±2.3%. The space cooling capacity increase percentage is beyond the measurement uncertainty. In the developed heat pump system, a refrigerant amount of 1.25 kg is charged in the refrigeration cycle.

3.2. Performance Analysis of the System in the Space Cooling Mode

In the SC operational mode, the heat pump operates at outdoor T_{db} and T_{wb} levels of 35 °C and 25.6 °C, respectively, and the operational parameter values of the discharging temperature, high refrigerant pressure, low refrigerant pressure, superheat degree and power consumption of the compressor in the refrigeration cycle are 83.5 °C, 31.9 kg/cm^2, 10.5 kg/cm^2, 7.8 °C and 1.63 kW, respectively. Under these operational conditions and operational parameters, the SC capacity and $COP_{s,c}$ of the system reach 4.1 kW and 2.52, respectively.

Table 4 lists the operational conditions, operational parameters and corresponding performance of the developed system in the SC, SH, WH, WC, SC/WH and SH/WH operational modes.

Table 4. Operational conditions and performance of the developed heat pump in the space cooling and heating operational modes.

Items	Unit	SC	SH	WH	WC	SC, WH	SH, WH
indoor T_{db}	°C	27.0	20.0	20.0	-	27.0	20.0
indoor T_{wb}	°C	19.0	15.0	15.0	-	19.0	15.0
T_{db} of indoor supply air	°C	15.7	31	-	-	17.3	26.0
outdoor T_{db}	°C	35	7.1	-	35.0	22.7	7.1
outdoor T_{wb}	°C	25.6	5.97	-	24.0	19.8	6.0
T_{db} of outdoor supply air	°C	46.9	3.3	13.1	43.3	24.0	6.4
water Inlet Temperature	°C	-	-	15.4	12.0	15.2	9.2
water outlet Temperature	°C	-	-	54.5	7.4	54.3	30.8
hot water flow rate	LPM	-	-	2.1	-	2.1	2.1
Chilled water flow rate	LPM	-	-	-	8.2	-	-
discharge temperature	°C	83.5	70.1	85.3	81.8	85.3	84.3
suction temperature	°C	18.1	0.6	8.75	4.5	12.6	14.2
high-pressure	kg/cm^2	31.9	24.8	37.1	28.1	38.5	19.6
low-pressure	kg/cm^2	10.5	7.8	10.0	7.1	11.4	5.4
mass flow rate 1	kg/h	110.1	111.7	124.3	94.7	120.1	73.8
mass flow rate 2	kg/h	-	-	76.9	-	-	21.6
superheat degree	°C	7.8	3.4	1.1	7.7	7.8	23.6
air volume	m^3/h	873.06	1002.35	-	-	906.25	1013.24
operation power	kW	1.63	1.35	1.8	1.4	1.8	1.5
Space heating capacity/cooling capacity	kW	4.1	3.56	-	-	3.2	2.0
Water heating capacity/cooling capacity	kW	-	-	5.7	2.7	5.0	0.9
$COP_{s,c}$ /$COP_{s,h}$/$COP_{w,h}$/$COP_{w,c}$	W/W	2.52	2.63	3.19	1.93	1.81/2.77	1.36/0.66
$COP_{t,sc/wh}$/$COP_{t,sh/wh}$	-	-	-	-	-	4.58	2.02

3.3. Performance Analysis of the System in the Space Heating Mode

In the SH operational mode, the heat pump operates at outdoor T_{db} and T_{wb} levels of 7.1 °C and 5.97 °C, respectively, and the operational parameter values of the discharging temperature, high refrigerant pressure, low refrigerant pressure, superheat degree and power consumption of the compressor in the refrigeration cycle are 70.1 °C, 24.8 kg/cm^2, 7.8 kg/cm^2, 3.4 °C and 1.35 kW, respectively. Under these operational conditions and operational parameters, the SH capacity and $COP_{s,h}$ of the system can reach 3.56 kW and 2.63, respectively.

3.4. Performance Analysis of the System in the Water Heating Mode

The operational conditions, operational parameters and corresponding performance of the developed system in WH mode are listed in Table 4. The heat pump operates at indoor T_{db} and T_{wb} levels of 20 °C and 15 °C, respectively, and the water is directly heated from 15.4 °C to 54.5 °C at a flow rate of 2.1 LPM by the plate heat exchanger. In the refrigeration cycle, the superheat degree is 1.1 °C, the discharging temperature is 85.3 °C, and the compressor power consumption is 1.8 kW.

Under the above operational conditions and operational parameters, the *COP* for WH ($COP_{w,h}$) and WH capacity reach values of 3.19 and 5.7 kW, respectively.

3.5. Performance Analysis of the System in the Water Cooling Mode

The performance of the system is investigated in the WC mode in an environment at an outdoor T_{db} level of 35 °C and an outdoor T_{wb} level of 24 °C. The supplied water temperature to the PHX I for cooling is 12°C, and the discharging water temperature from the plate heat exchanger is 7.4 °C with a water temperature difference of approximately 4.7 °C. The average cooling capacity reaches a value of 2.7 W with a *COP* for WC, i.e., a $COP_{w,c}$, of 1.93.

3.6. Performance Analysis of the System in the Composite Operational Mode

The developed system can perform in two composite operational modes, namely, the SH/WH composite mode and the SC/WH composite mode. In the SC/WH mode, cold air and hot water can be simultaneously supplied, while warm air and hot water can be simultaneously generated in the SH/WH mode. The performance of the developed system in the SC/WH operational mode was measured at an indoor T_{db} level of 27 °C and T_{wb} of 19 °C. However, the performance in the SH/WH operational mode was measured at an indoor T_{db} level of 27 °C and T_{wb} of 15 °C and an outdoor T_{db} level of 7 °C and T_{wb} of 6 °C. The circulating water from the tank is heated directly to 55 °C by plate heat exchanger II in the SC/WH composite mode with an initial water temperature of 15 °C, but it is directly heated to 55 °C from an initial water temperature of 9 °C in the tank in the SH/WHC composite operational mode, as summarized in Table 5.

Table 5. Operational environments for the two composite operational modes.

Items	Indoor Temperature (°C)	Outdoor Temperature (°C)	Water Inlet Temperatures (°C)	Water Outlet Temperatures (°C)
Air Cooling and Water Heating	T_{db} = 27 °C T_{wb} = 19 °C	–	15 °C	55 °C
Air Heating and Water Heating	T_{db} = 20 °C T_{wb} = 15 °C	T_{db} = 7 °C T_{wb} = 6 °C	9 °C	55 °C

According to the experimental results in Table 4, in the SC/WH composite mode, the average SC capacity reached 3.2 kW, and the average WH capacity reached 5.0 kW. The values of $COP_{s,c}$, $COP_{w,h}$ and $COP_{t,sc/wh}$ reach 1.81, 2.77 and 4.58, respectively. However, in the SH/WH composite mode, the average SH capacity reaches 2.0 kW, while the average WH capacity reaches 0.9 kW. The values of $COP_{s,h}$, $COP_{w,h}$ and $COP_{t,sh/wh}$ reach 1.36, 0.66 and 2.02, respectively. In the SH/WH composite mode, the total heat absorbed from FTHX I and from the operational compressor has to be allocated to both PHX II and FTHX II for heat recovery. Thus, the SH capacity due to FTHX II and the water heating capacity due to PHX II are lower than the water heating capacity in the SC and WH composite mode. Furthermore, to attain the required hot water temperature of 55 °C at the outlet of high-pressure PHX II, the openness of the electronic expansion valve is decreased to reduce the mass flow rate of the refrigerant in the refrigeration cycle, and the retention time for the refrigerant in PHX II can increase. Thus, a high superheat degree and high discharging temperature can be obtained, as indicated in Table 5.

The P-h diagrams for each operational mode in terms of the measurement conditions in Table 4 are shown in Figures 6–8.

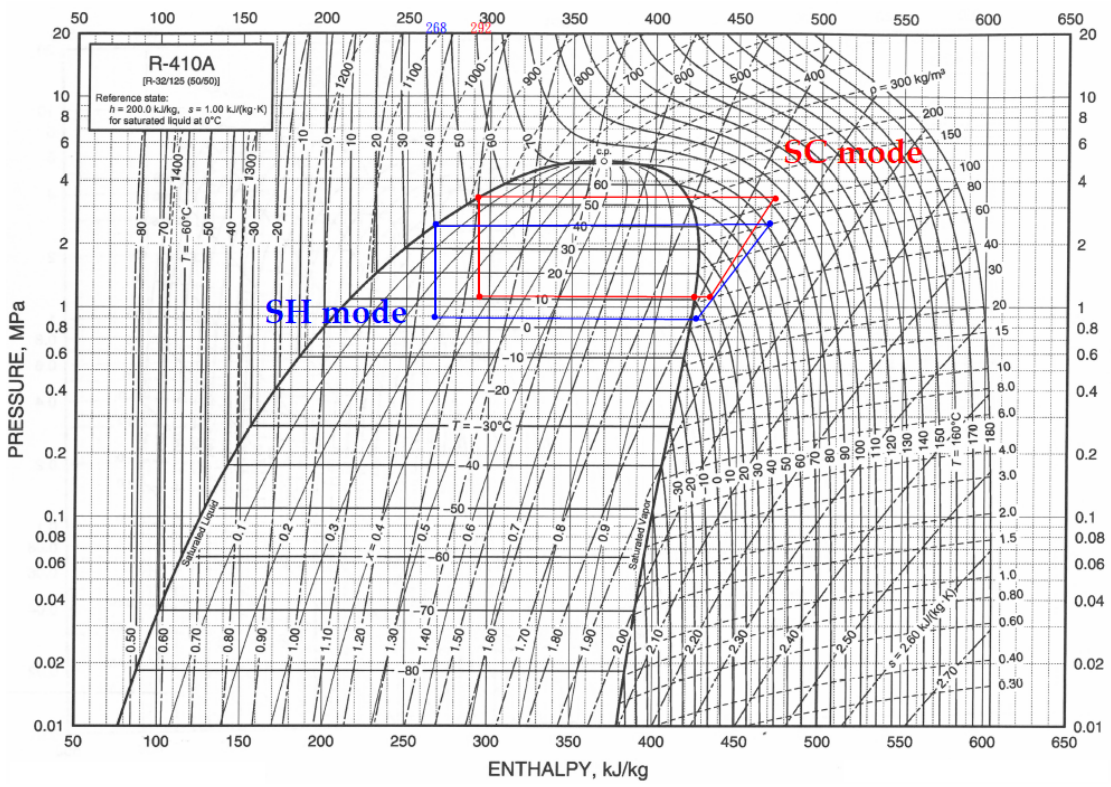

Figure 6. Log P-h diagram of the SC mode and SH mode for the refrigerant.

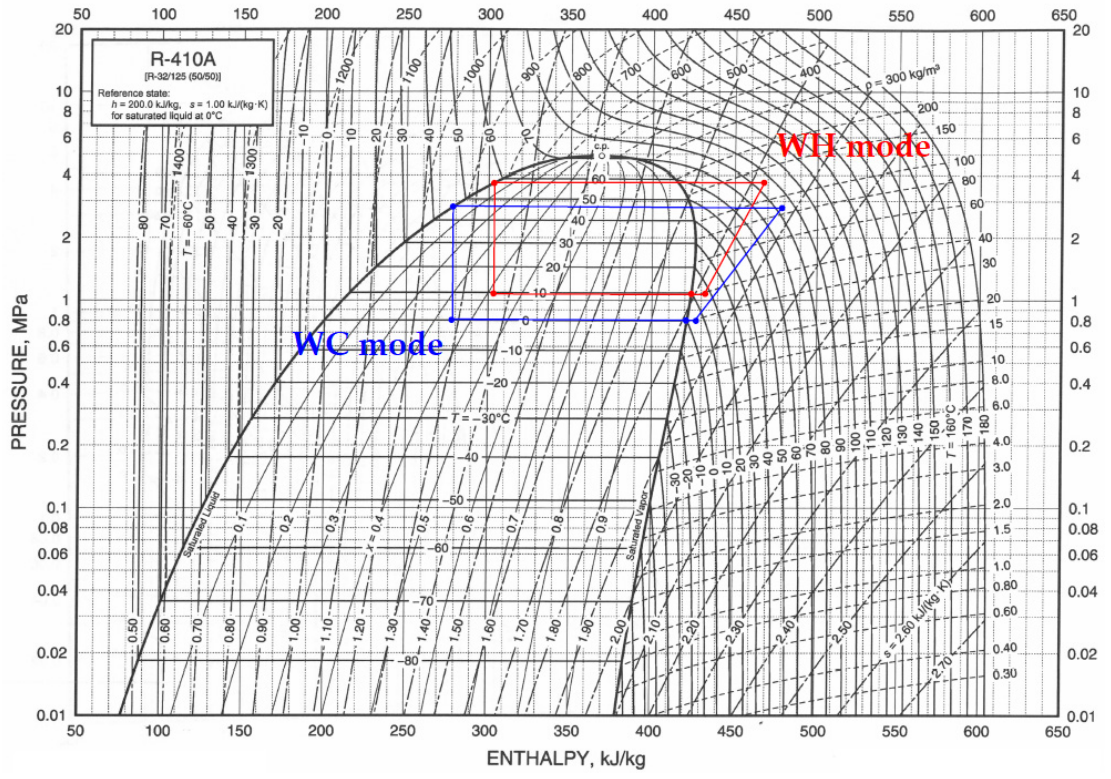

Figure 7. Log P-h diagram of the WH mode and WC mode for the refrigerant.

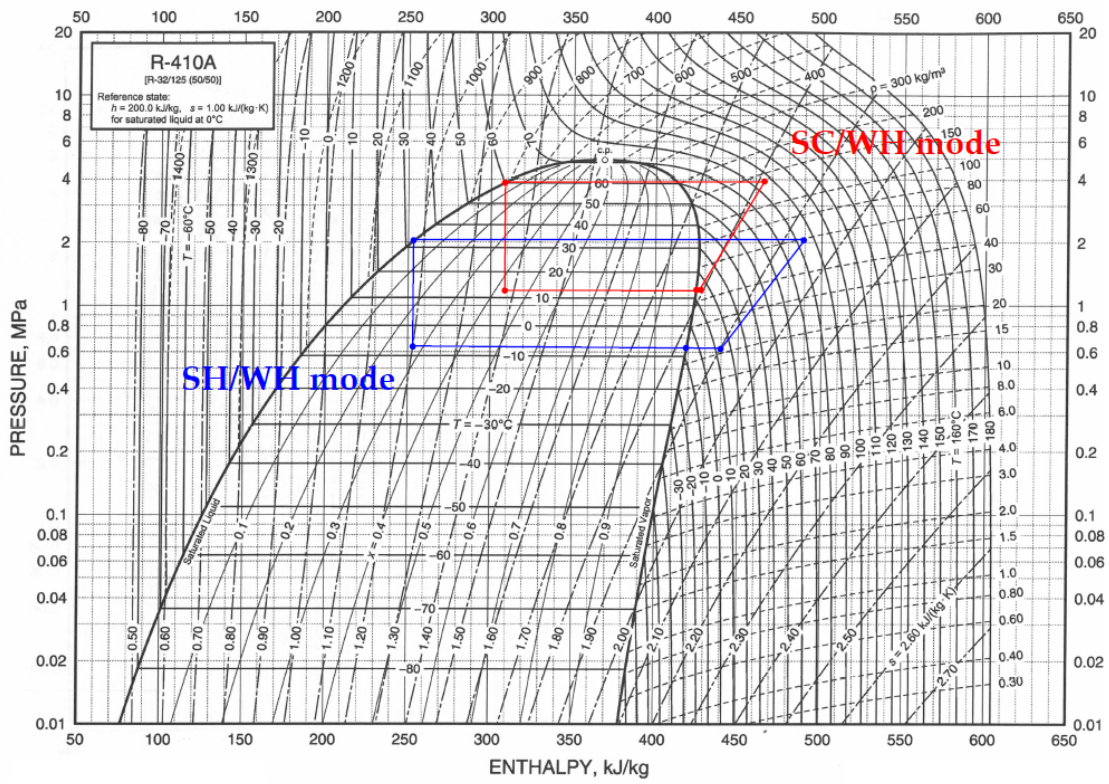

Figure 8. Log P-h diagram of the SC/WH mode and SH/WH mode for the refrigerant.

Figures 6–8 illustrate the corresponding refrigeration cycles on R410A pressure-enthalpy (Log p-h) diagram for different operational modes of the developed system. The refrigeration cycles on the Log p-h diagram are constructed in terms of the high pressure, low pressure, suction temperature and discharge temperature of each operational mode in Table 4. The pressure drops, thermal resistances and compressing efficiency in the refrigeration cycle are neglected. From the refrigeration cycles, the $COP_{s,c}$ is about 3.88, the $COP_{s,h}$ is 3.42, the $COP_{w,h}$ is 3.36 and the $COP_{w,c}$ is 2.7. For the composite operational modes, the $COP_{s,c}$ of SC/WH operational mode is about 3.22. However, for the SH/WH operational mode, the discharge refrigerant vapor from the compressor is allocated to PHX I and FTHX II for water and space heating, the refrigerant flow rates in the two heat exchangers are less in comparison to those in the other operational modes. Thus, the high pressure and low pressure in the refrigeration cycle are less than those in the operational modes, which make the generating hot water from PHX I only attain about 38 °C, as shown in Table 4. In SH/WH operational mode, the $COP_{s,h}$ is estimated to be 3.41. The space heating/cooling capacity and water heating/cooling capacity based on Log p-h diagrams are calculated as shown in Table 6. The results in Table 6 from theoretical analysis can be used to justify the experimental results in Table 4.

Table 6. Space heating/cooling capacity and water heating/cooling capacity based on Log p-h diagrams.

Mode	SC	SH	WH	WC	SC/WH	SH/WH
Space heating capacity/ cooling capacity	4.28	4.81	-	-	4.17	2.83
Water heating capacity/cooling capacity	-	-	5.80	3.82	5.33	1.17

In Figure 9, comparing the values of $COP_{w,h}$ and $COP_{s,c}$ of the developed system in the WH mode, SC mode and SC/WH composite mode, in terms of WH, the value of $COP_{w,h}$ in the composite operational mode is 14% lower than that in the WH mode, and the WH capacity in the composite mode

can attain a value of 5 kW as well. Regarding SC, the value of $COP_{s,c}$ in the composite operational mode is lower than that in the SC mode as well under the same operational conditions at an outdoor T_{db} level of 27 °C.

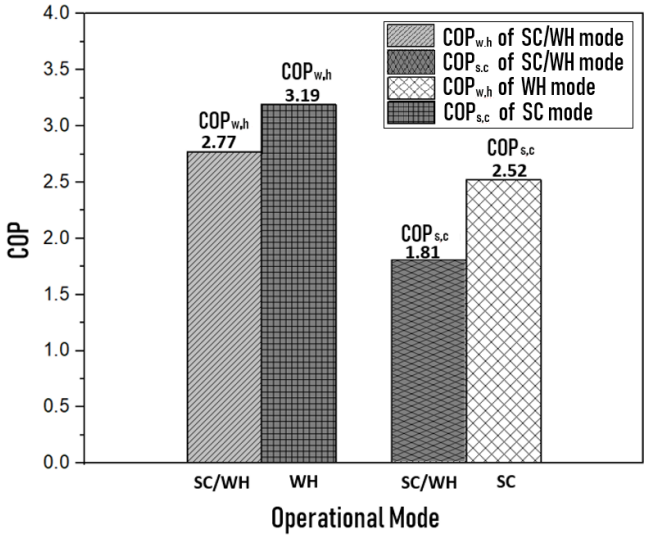

Figure 9. *COP* value comparison among the water heating mode, space cooling mode and water heating/space cooling composite mode.

Figure 10 compares the coefficients of the performance for WH and SH of the developed system among the SH/WH composite mode, WH mode and SH operational mode. In the SH/WH composite mode, because the total heat absorbed from the low-pressure FTHX I and from the operational compressor has to be allocated to both the high-pressure PHX II and FTHX II for heat recovery, the space heating capacity of the FTHX II and the water heating capacity of the PHX II are lower than those in the space cooling mode and water heating mode, respectively. Thus, the values of $COP_{w,h}$ and $COP_{s,h}$ in the composite mode are much lower than those in the WH mode and SH mode, respectively.

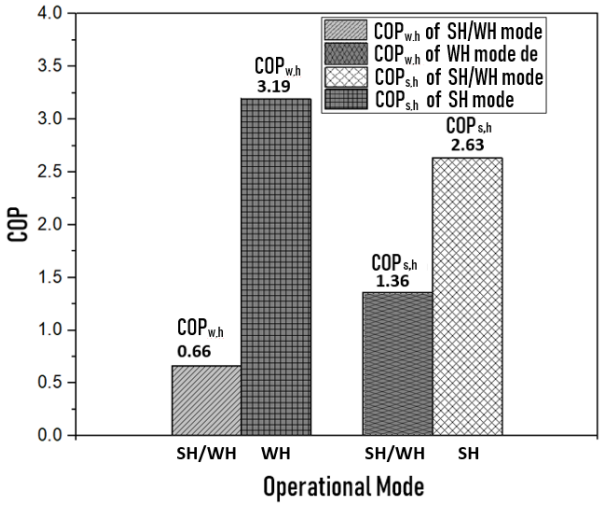

Figure 10. *COP* value comparison among the WH mode, SH mode and SH/WH composite mode.

The WH performance of the developed heat pump system in the WH mode was investigated at different ambient temperatures from 20 °C to 40 °C at intervals of 5 °C. According to the test standards of CNS 15466 and GB/T 21362, ambient thermostates of T_{db} = 5 °C and T_{wb} = 3 °C and T_{db} = 43 °C and T_{wb} = 26 °C are selected. Six thermostates on the straight line connecting the two above thermostates are defined at temperature intervals of 5 °C. The water heating performances of

the developed heat pump system in the WH mode at the different ambient temperatures are shown in Figure 11. At an ambient temperature of T_{db} = 5 °C, a lower evaporating temperature has to be attained in the FTHX I to gain the required heat from the ambient environment, and the refrigerant flow volume in the refrigeration cycle is smaller due to a larger refrigerant specific volume at the low evaporating temperature, which may lead to a lower heating capacity, but a higher power consumption of the compressor. Thus, the $COP_{w,h}$ at an ambient temperature of T_{db} = 5 °C is approximately 2.49. However, with increasing ambient temperature, the evaporating temperature and refrigerant flow volume in the refrigeration cycle increase as well, which causes a reduction in the power consumption of the compressor and an increase in the heating capacity. When the ambient temperature reaches T_{db} = 40 °C, the $COP_{w,h}$ of the system reaches a value of 4.12.

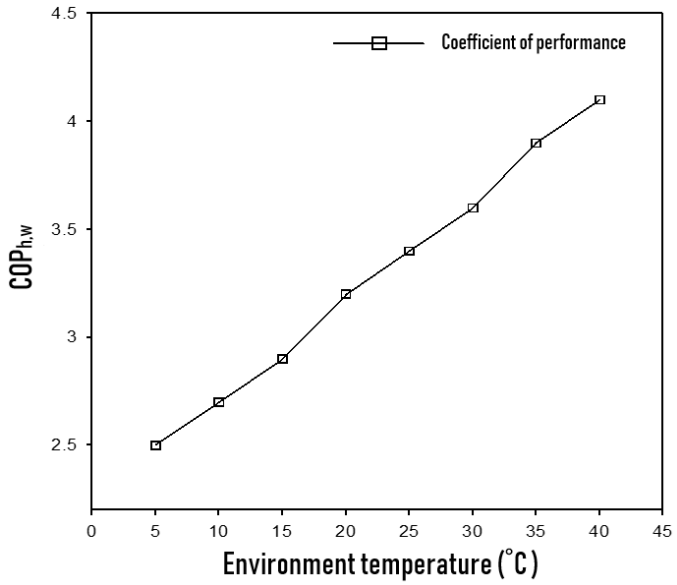

Figure 11. Water heating performance of the developed heat pump system in the WH mode at the different ambient temperatures.

3.7. Effect of Water Heating Methods on Water Heating Performance

Figure 12 shows the water heating capacity, compressor power consumption and circulating water flow rate of the developed system in the WH mode with the DWH and CWH methods based on the measurement standard of CNS 15466. The water from a 200 L water tank is introduced into the PHX II to recover heat from the refrigeration cycle with an initial temperature of 15 °C. In the DWH method, the supplied water in the PHX II is directly heated to the outlet temperature of each water heating stage in the plate heat exchanger by adjusting the introduced circulating water flow rate. However, in the CWH method, the supplied water flow rate to the PHX II is maintained at 14.75 LPM, and the outlet water temperature of the PHX II gradually rises with the heating time until the water temperature in the tank reaches the final temperature of each water heating stage.

Figure 12 and Table 7 show that with increasing water temperature in the water tank, the flow rate of the circulating water in the case with the CWH method remains at an almost constant value of 14.75 LMP. However, the circulating water flow rate in the case with the DWH method gradually decreases from a flow rate of 17.92 LMP to 13.12 LMP to attain the desired water temperature at each heating stage at the outlet of the PHX II. Regarding the water heating capacity, the water heating capacities in both cases gradually decrease with increasing water temperature at each water heating stage due to the gradual increase in condensation temperature. However, the water heating capacity in the case with the DWH method is higher than that in the case with the CWH method because a larger average water temperature difference occurs between the outlet and inlet of the PHX II and a higher water flow rate in the case with the DWH method is introduced. In terms of the power

consumption of the compressor, due to the rise in the condensation pressure in the refrigeration cycle with increasing water temperature in the tank, the power consumption of the compressor gradually increases with increasing the water heating stage in the tank as well. However, the power consumption of the compressor in both cases remains quite similar at the different water temperatures in the tank. Because of the higher heating capacity and similar power consumption of the compressor with the DWH method than that in the case with the CWH method, the values of $COP_{w,h}$ in the case with the DWH method at each heating stage are higher than those in the case with the CWH method.

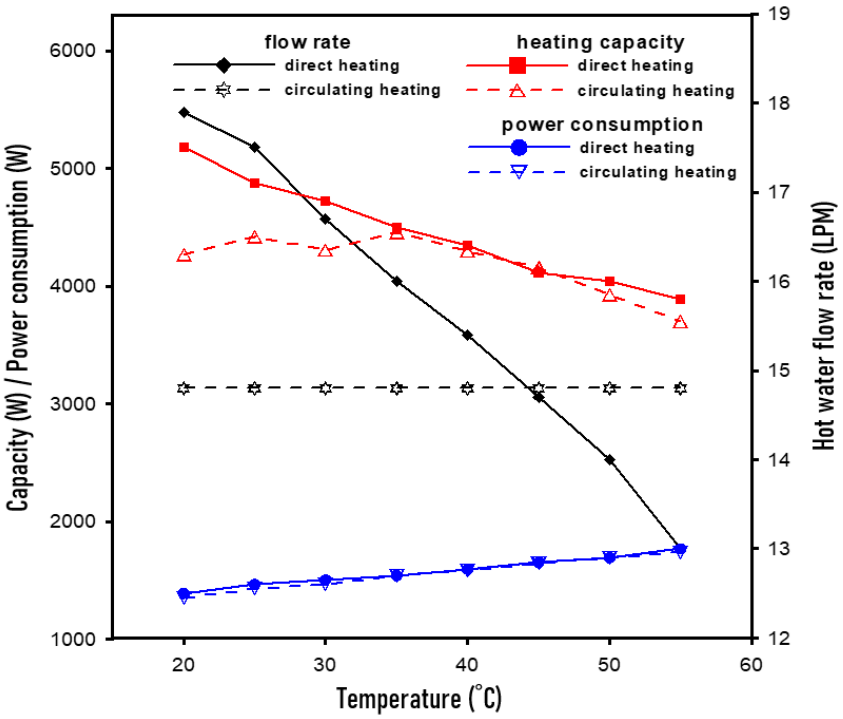

Figure 12. Comparison of the water heating capacity of the direct and circulating water heating methods.

Table 7. Water heating capacity and coefficient of performance with the different heating methods.

		Direct Heating Method (DWH)			Circulating Heating Method (CWH)				Improvement (%)	
Water Heating by PHX II		Water Heating Capacity (W)	$COP_{w,h}$ (W/W)	Hot Water Flow Rate (LPM)	Water Temperature in The Tank		Water Heating Capacity (W)	$COP_{w,h}$ (W/W)	Water Heating Capacity	$COP_{w,h}$
Inlet Temperature	Outlet Temperature				Initial	Final				
15 °C	20 °C	5989.79	4.53	17.92	15 °C	20 °C	4906.7	3.948	22.1	14.7
20 °C	25 °C	5685.78	4.03	17.48	20 °C	25 °C	5092.9	3.835	11.6	50.8
25 °C	30 °C	5502.43	3.83	16.67	25 °C	30 °C	4979.2	3.542	10.5	8.1
30 °C	35 °C	5281.38	3.56	15.96	30 °C	35 °C	5146.2	3.453	2.6	3.1
35 °C	40 °C	5172.35	3.21	15.26	35 °C	40 °C	4956.1	3.121	4.3	2.9
40 °C	45 °C	4803.16	2.83	14.5	40 °C	45 °C	4838.6	2.85	0.0	0.0
45 °C	50 °C	4743.26	2.60	14.07	45 °C	50 °C	4550	2.51	4.2	3.6
50 °C	55 °C	4446.71	2.27	13.12	50 °C	55 °C	4246.7	2.19	4.7	3.7
15 °C	55 °C	5715.17	3.19	2.1	15 °C	55 °C	4812.1	3.06	18.8	4.2

3.8. Refrigerant Pressure Build-Up during Operational Mode Switching

In the refrigerant piping design of the developed multifunctional heat pump system, the plate heat exchanger and fin-tube heat exchanger are arranged in parallel. When the operational function is switched from one operational mode to another mode, refrigerant pressure build-up in the refrigeration cycle and refrigeration oil deposition in the heat exchangers are two major problems that need to be considered. The pump-down method is usually applied to collect any deposited refrigeration oil in the condenser before operational mode switching, which is beneficial to the refrigerant pressure difference build-up after operational mode switching and avoids refrigerant oil deposition in the heat exchangers, resulting in insufficient oil in the compressor. In this study, a refrigerant pressure balance control method for refrigerant pressure build-up in the refrigeration cycle during operational mode switching is proposed, in which, before operational mode switching, all solenoid valves and expansion valves are fully open for a while, thus acting as solenoid valves in terms of operational mode switching. In this study, the refrigerant mass flow rates in the refrigerant cycle and required time for the refrigerant after operational mode switching by the pump-down method and the proposed refrigerant pressure balance method are investigated.

Figure 13 shows the refrigerant mass flow rate after switching to the different operational modes from the SC mode by the pressure balance method and pump-down method at an environment temperature of 24 °C. After switching modes, the tank is heated from 30 °C to 55 °C under the DWH method. The refrigerant mass flow rates in the discharging line of the compressor after attaining the steady state are 120 kg/h and 124 kg/h by the pressure balance method and pump-down method, respectively. The deviation between the mass flow rates in the discharging line is quite small. The required heating times for water to reach 55 °C are 28 min and 24 min by the pressure balance method and pump-down method, respectively. From the above results in terms of the required heating time and refrigerant mass flow rate, the deviations of the experimental results between the two control methods are quite small.

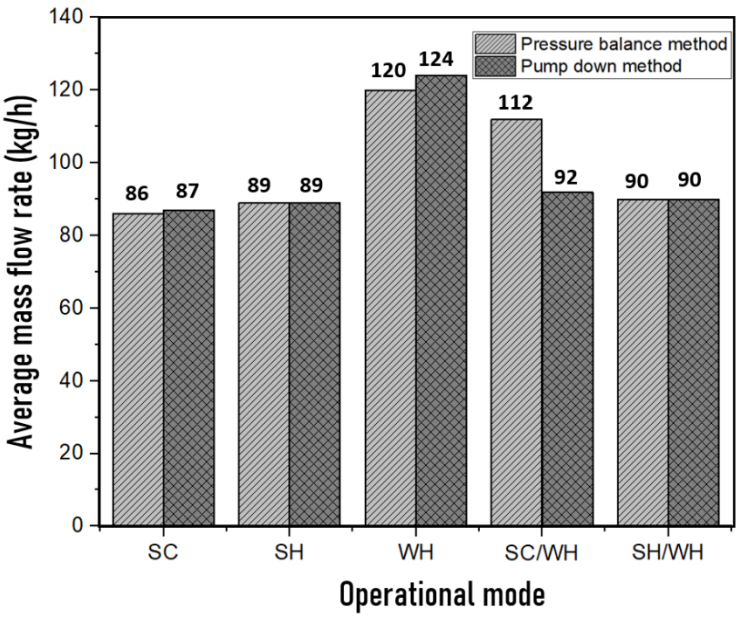

Figure 13. Refrigerant mass flow rate in the refrigeration cycle after switching to a different operational mode from the space cooling mode at an environment temperature of 24 °C.

In Figure 13, the refrigerant mass flow rates in the refrigeration cycle are shown after switching to the SC/WH composite operational mode from the SC mode at an environment temperature of 24 °C. The water in the storage tank is heated from 30 °C to 55 °C by the DWH method. According to the experimental results, after the system reaches the steady state, the average supplied air temperatures

by the pressure balance method and pump-down method are 22.5 °C and 25.4 °C, respectively. Figure 13 shows that the refrigerant mass flow rate in the discharging line of the compressor by the pressure balance method is 112 kg/h, which is higher than the value of 92 kg/h by the pump-down method. The refrigerant mass flow rate in the PHX II of 92 kg/h by the pressure balance method is higher than the value of 85 kg/h by the pump-down method. Under the pump-down method, most of the refrigerant is collected in the FTHX II. At the moment of operational mode switching, a longer time is required to allocate the refrigerant flows in the PHX II and the FTHX II and build up the high and low refrigerant pressures in the refrigeration cycle. Thus, regarding the required times to heat the water to 55 °C, a heating time of 35 min is required by the pressure balance method, but 75 min of heating are required by the pump-down method. Thus, in the parallel refrigerant piping arrangement and composite operational mode, the pressure balance method is a suitable switching method for operational mode switching.

Figure 13 shows the refrigerant mass flow rates in the refrigeration cycle after switching to the SH/WH composite operational mode from the SC mode at an environment temperature of 24 °C. The water in the storage tank is heated from 30 °C to 55 °C under the DWH method. From the experimental results, after the system reaches the steady state, the average supplied air temperatures by the pressure balance method and pump-down method are 33.1 °C and 34 °C, respectively. Figure 13 reveals that the refrigerant mass flow rates in the discharging line of the compressor by both the pressure balance method and the pump-down method are 90 kg/h. The refrigerant mass flow rate of 41 kg/h in the FTHX I by the pressure balance method is slightly lower than the value of 42 kg/h by the pump-down method. At the moment of operational mode switching, most refrigerant vapor from the compressor discharging line flows into the FTHX I, which leads to a higher supplied air temperature in the air-conditioning space.

4. Conclusions

In this study, a multifunctional heat pump system offering six different operational modes with parallel refrigerant piping design is developed in order to cover more evaporation and condensation heat from the refrigeration cycle. The performance of the developed heat pump system in the different operational modes is investigated at different environment temperatures. Moreover, the effect of water heating methods and refrigerant pressure build-up methods on the performance of the developed system is investigated as well.

From the experimental results, it can be seen that the performances of the developed system in different operational modes are similar to the single functional heat pump system, except the space heating and water heating composite operational mode. In the space heating and water heating composite operational mode, the discharge refrigerant vapor from the compressor has to allocate to the fin-tube heat exchanger I and the plate heat exchanger II for space heating and water heating. Thus, the space heating capacity and water heating capacity are lower than those of the other spacing heating and water heating operational mode. Moreover, the refrigerant vapor flow rates in the fin-tube heat exchanger I and the plate heat exchanger II, depending on the flow resistances in the two heat exchangers, cannot be controlled by the actions of on-off valves. This leads to the water heating capacity and space heating capacity in the composite operational mode depending on the flow resistances in the two heat exchangers as well.

Moreover, the effect of the direct water heating method and circulating water heating method on the water heating performance of the system was investigated. It was found that the water heating performance of the system by the direct water heating method is better than that of the system by the circulating water heating method. The water heating capacity and water heating coefficient of performance of the direct water heating method can be improvement by 2.6% to 22.1% and 2.9% to 50.8%, respectively.

Finally, a refrigerant pressure balance method is proposed in the study to build up the pressure difference in the refrigeration cycle. In the space cooling and water heating composite mode, the required heating time can be greatly reduced by the proposed refrigerant pressure balance method.

The developed multifunctional heat pump system can find broad applications in households, hospitals, hotels, schools, swimming pools, nursing homes, food and industry manufacturing processes for space cooling/heating and hot/chilled water generations. The present developed multifunctional heat pump system consists of two fin-tube heat exchangers, two plate heat exchangers, two electronic expansion valves, one four-way valve and several solenoid valves in order to perform different valve actions and require operational modes. Reducing the required units of solenoid valves and simplifying the required operational actions of solenoid valves are the possible topics of future study.

Author Contributions: Research concept was proposed by W.J.L. and K.Y.L.; Data processing and the manuscript preparation were conducted by K.Y.L., J.M.H. and C.K.Y.; Data analysis and interpretation were implemented by W.J.L., K.Y.L., C.K.Y. and J.M.H.; Manuscript editing was performed by W.J.L., and K.Y.L. All authors have read and agreed to the published version of the manuscript.

Funding: This research was funded by the Ministry of Science and Technology of Taiwan under grant number MOST 103-2622-E-167-019-CC3 and MOST 107-2221-E-167-020.

Acknowledgments: The authors gratefully acknowledge the financial support provided to this study by the Ministry of Science and Technology of Taiwan under Grant MOST 103-2622-E-167-019-CC3 and MOST 107-2221-E-167-020.

Conflicts of Interest: The authors declare no conflict of interest.

Glossary

Nomenclature

CWH	circulating water heating	SC	Space cooling mode
COP	Coefficient of performance	SC/WH	Space cooling and water heating mode
C_p	Specific heat of water, J/kg*K	SH	Space heating mode
FTHX	Fin-tube heat exchanger	SH/WH	Space heating and water heating mode
$\dot{m}$	Flow rates, kg/h	SV	Refrigerant control valve
MFR	Refrigerant mass flowmeter	*T*	Temperature, °C
PHX	The plate heat exchanger	V	Pipeline valve
Q	Instant capacity, kW	*W*	Instant required power for the compressor
WC	Water cooling mode	WH	Water heating mode
τ	Operating period of duration		

Subscript

db	Dry bulb	*sho*	Air at the outlet of the FTHX in space heating
s, *c*	Space cooling	*wb*	Wet bulb
sc/*wh*	Space cooling/water heating	*w*, *c*	Water cooling
sci	Air at the inlet of the FTHX in space cooling	*wci*	Water at the inlet of the PHX in water cooling
sco	Air at the outlet of the FTHX in space cooling	*wco*	Water at the outlet of the PHX in water cooling
s, *h*	Space heating	*w*, *h*	Water heating
sh/*wh*	Space heating/water heating	*whi*	Water at the inlet of the PHX in water heating
shi	Air at the inlet of the FTHX in space heating	*who*	Water at the outlet of the PHX in water heating
t	Total		

References

1. Hepbasli, A.; Kalinci, Y. A Review of Heat Pump Water Heating Systems. *Renew. Sustain. Energy Rev.* **2009**, *13*, 1211–1229. [CrossRef]
2. Luo, W.J.; Faridah, D.; Fasya, F.R.; Chen, Y.S.; Mulki, F.H. Performance Enhancement of Hybrid Solid Desiccant Cooling Systems by Integrating Solar Water Collectors in Taiwan. *Energies* **2019**, *12*, 3470. [CrossRef]
3. Ahmadi, G.; Toghraie, D.; Azimian, A.; Akbari, O.A. Evaluation of Synchronous Execution of Full Repowering and Solar Assisting in a 200 MW Steam Power Plant, a Case Study. *Appl. Therm. Eng.* **2017**, *112*, 111–123. [CrossRef]
4. Barnoon, P.; Toghraie, D. Numerical Investigation of Laminar Flow and Heat Transfer of Non-Newtonian Nanofluid within a Porous Medium. *Powder Technol.* **2018**, *325*, 78–91. [CrossRef]
5. Liu, X.; Ni, L.; Lau, S.K.; Li, H. Performance Analysis of a Multi-Functional Heat Pump System in Heating Mode. *Appl. Therm. Eng.* **2013**, *51*, 698–710. [CrossRef]
6. Sozen, A.; Altıparmak, D.; Usta, H. Development and Testing of a Prototype of Absorption Heat Pump System Operated by Solar Energy. *Appl. Therm. Eng.* **2002**, *22*, 1847–1859. [CrossRef]
7. Lai, J.C.; Luo, W.J.; Wu, J.Y. Performance Analysis of Single-Stage Air Source Heat Pump Utilizing Indirect Vapor Injection Design. *Adv. Mech. Eng.* **2018**, *10*, 1687814018767487. [CrossRef]
8. Ma, X.; Chen, J.; Li, S.; Sha, Q.; Liang, A.; Li, W.; Zhang, J.; Zheng, G.; Feng, Z. Application of Absorption Heat Transformer to Recover Waste Heat from a Synthetic Rubber Plant. *Appl. Therm. Eng.* **2003**, *23*, 797–806. [CrossRef]
9. Yao, Y.; Jiang, Y.; Deng, S.; Ma, Z. A Study on the Performance of the Airside Heat Exchanger under Frosting in an Air Source Heat Pump Water Heater/Chiller Unit. *Int. J. Heat Mass Transf.* **2004**, *47*, 3745–3756. [CrossRef]
10. Ding, Y.; Chai, Q.; Ma, G.; Jiang, Y. Experimental Study of an Improved Air Source Heat Pump. *Energy Convers. Manag.* **2004**, *45*, 2393–2403. [CrossRef]
11. Lu, S.; Wu, J.Y. Optimal Selection among Different Domestic Energy Consumption Patterns Based on Energy and Exergy Analysis. *Energy Convers. Manag.* **2010**, *51*, 1398–1406. [CrossRef]
12. Chang, C.C.; Luo, W.J.; Lu, C.W.; Cheng, Y.S.; Tsai, B.Y.; Lin, Z.H. Effects of Process Air Conditions and Switching Cycle Period on Dehumidification Performance of Desiccant-Coated Heat Exchangers. *Sci. Technol. Built Environ.* **2017**, *23*, 81–90. [CrossRef]
13. Hiltunen, P.; Syri, S. Highly Renewable District Heat for Espoo Utilizing Waste Heat Sources. *Enerigies* **2020**, *13*, 3551. [CrossRef]
14. Gong, G.; Zeng, W.; Wang, L.; Wu, C. A New Heat Recovery Technique for Air-Conditioning/Heat-Pump System. *Appl. Therm. Eng.* **2008**, *28*, 2360–2370. [CrossRef]
15. Liu, H.; Nagano, K.; Katsura, T.; Han, Y. Experimental Investigation on a Vapor Injection Heat Pump System with a Single-Stage Compressor. *Enerigies* **2020**, *13*, 3133. [CrossRef]
16. León-Ruiz, J.E.D.; Carvajal-Mariscal, I. Mathematical Thermal Modelling of a Direct-Expansion Solar-Assisted Heat Pump Using Multi Objective Optimization Based on the Energy Demand. *Enerigies* **2018**, *11*, 1773. [CrossRef]
17. Xu, J.; Zhao, Y.; Quan, Z.; Wang, G.; Wang, J. Air–Water Dual-Source Heat Pump System with New Composite Evaporator. *Appl. Therm. Eng.* **2017**, *141*, 483–493. [CrossRef]
18. Liu, Z.; Lou, F.; Qi, X.; Shen, Y. Enhancing Heating Performance of Low-Temperature Air Source Heat Pumps Using Compressor Casing Thermal Storage. *Enerigies* **2020**, *13*, 3269. [CrossRef]
19. Ji, J.; Pei, G.; Chow, T.T.; He, W.; Zhang, A.; Dong, J.; Yi, H. Performance of Multi-Functional Domestic Heat-Pump System. *Appl. Energy* **2005**, *80*, 307–326. [CrossRef]
20. Liang, C.H.; Wen, X.T.; Zhang, X.S.; Xiao, H.H. Experimental Study on the Performance of Multifunction Heat Pump for Domestic Hot Water. In Proceedings of the 2011 International Conference on Electric Technology and Civil Engineering (ICETCE), Lushan, China, 22–24 April 2011; pp. 3166–3168.
21. Liu, X.; Lau, S.K.; Li, H.; Shen, H. Optimization and Analysis of a Multi-Functional Heat Pump System with Air Source and Gray Water Source in Cooling Mode. *Energy Build.* **2017**, *149*, 339–353. [CrossRef]
22. Liu, X.; Hui, F.; Guo, Q.; Zhang, Y.; Sun, T. Experimental Study of a New Multifunctional Water Source Heat Pump System. *Energy Build.* **2016**, *111*, 408–423. [CrossRef]

23. Liu, X.; Ni, L.; Lau, S.K.; Li, H. Performance Analysis of a Multi-Functional Heat Pump System in Cooling Mode. *Appl. Therm. Eng.* **2013**, *59*, 253–266. [CrossRef]
24. Luo, W.J.; Kuo, H.C.; Wu, J.Y.; Faridah, D. Development and Analysis of a New Multi-Function Heat Recovery Split Air Conditioner with Parallel Refrigerant Pipe. *Adv. Mech. Eng.* **2016**, *8*, 1687814016671444. [CrossRef]
25. Kline, J.; McClintock, F.A. Describing uncertainties in single sample experiments. *Mech. Eng.* **1953**, *1*, 3–9.